Computers and Concrete, *Vol. 17, No. 6 (2016) 703-721*
DOI: http://dx.doi.org/10.12989/cac.2016.17.6.703

Layered model of aging concrete. General concept and one-dimensional applications

Andrzej Truty*, Jan Szarliński[a] and Krzysztof Podleś[b]

Department of Environmental Engineering, Cracow University of Technology, ul. Warszawska 24, 31-155 Kraków, Poland

(Received April 23, 2015, Revised January 1, 2016, Accepted February 25, 2016)

Abstract. A novel approach to modeling concrete behavior at the stage of its maturing is presented in this paper. This approach assumes that at any point in the structure, concrete is composed of a set of layers that are activated in time layer by layer, based on amount of released heat that is produced during process of the concrete's maturing. This allows one to assume that each newly created layer has nominal stiffness moduli and tensile/compressive strengths. Hence introduction of explicit stiffness moduli and tensile/compressive strength dependencies on time, or equivalent time state parameter, is not needed. Analysis of plain concrete (PC) and reinforced concrete (RC) structures, especially massive ones, subjected to any kind of straining in their early stage of existence, mostly due to external loads but especially by thermal loading and shrinkage, is the goal of the approach. In this article a simple elasto-plastic softening model with creep is used for each layer and a general layered model behavior is illustrated on one-dimensional (1D) examples.

Keywords: concrete; aging; constitutive modeling

1. Introduction

The problem of degradation of concrete stiffness and strength, caused by straining, or even cracking, during the process of its maturing, is very important in ultimate (ULS) and serviceability (SLS) limit state analysis of massive structures. Concrete overstrained and damaged, even partly, in the period of its maturing, may affect those states in a significant way, and cause that the structure will be unable to fulfill conditions and requirements defined by engineers. Damage is irreversible and therefore cracked concrete at a given time instance of its maturing will not reach full tensile strength, which it would reach if it were not cracked. This results from an apparent fact that new bonds inside the concrete structure, created during further hydration process of cement after cracking, cannot arise through the crack, since its width exceeds multitudinously the distance between particles of the hydrated cement solid structure. In other words, bonds cannot grow through the crack and although the solid structure will grow in the whole region of the concrete's body, surrounding the crack, it will not be able to carry any tensile stresses. It is however known

*Corresponding author, Professor, E-mail: andrzej.truty@gmail.com
[a]Professor emeritus, E-mail: janszarlinski@poczta.neostrada.pl
[b]Ph.D., E-mail:kpodles@usk.pk.edu.pl

http://www.techno-press.org/?journal=cac&subpage=8 ISSN: 1598-8198 (Print), 1598-818X (Online)

that cracked concrete may exhibit the self-healing phenomenon caused by chemical reactions taking place between unhydrated cement and carbon dioxide (dissolved in the water for instance). This phenomenon is currently in the stage of intensive research as it may bring new techniques to be used for repairing damaged concrete structures (see for instance the report by Mihashi *et al.* (2012)).

The forgoing straining of concrete is, in principle, caused by stresses generated by imposed tensile strains arising in the course of cooling the concrete after it reaches the highest temperature during the hydration process. This phenomenon is very important and always present especially in such massive concrete structures as gravity dams or concrete elements of earth dams, supports of bridges, raft-pile slabs of high buildings and many other civil engineering structures. Considering serviceability state of cracks and deformation one can state that it is almost impossible to determine it for the structures in question using available designing methods, if they are overstrained in the period of the maturing. This problem is very important, because in most practical computations according to the EC2 the ultimate serviceability limit state is based on elastic computations for quasi-static combination of loads assuming effective stiffness moduli (creep coefficient is applied). Although for ordinary beams this approach seems to be simple and good enough for design, for massive reinforced concrete structures it is questionable, especially for large structures interacting with subsoil. Among the publications concerning modeling creep and aging of concrete the solidification theory proposed by Bažant *et al.* (1989a, b) is treated as a reference one. In this theory time dependence of elastic moduli is eliminated and authors introduce so-called volume fraction growth function that depends on time. This model assumes that the total strain increment is a sum of the elastic strain, creep strain being a sum of visco-elasticity and viscous flow, shrinkage and thermal strains, and cracking. The model, extended later on to the concept of micro-prestress theory presented by Bažant *et al.* (1997a, b) and Havlásek and Jirásek (2012), is able to explain additional creeping that appears after one year of the structure life. In several publications the solidification theory is supplied by an extensive study of all major effects connected to the hydro-thermal and hydration phenomena analyzed at the micro-scale and later on generalized to the macro-scale by means of averaging theory as proposed by Hassanizadeh and Gray (1979). Comprehensive proposals going in this direction are published mainly in papers by Gawin *et al.* (2006 a, b), but also in the PhD thesis by Havlásek (2014). An interesting paper in that matter was published by Mabrouk *et al.* (2004) where the model of concrete is a parallel composition of creeping layers. Similarly to the work by Gawin *et al.* (2006 a, b) the coupling between skeleton stresses and pore water pressure, by means of the effective stress principle, is taken into account. To complete the important bibliography in this matter one may emphasize the research by Witakowski (1998), concerning thermodynamic theory of concrete maturing. As it was mentioned above in many publications a deep insight is provided into the microstructure of maturing concrete, but in none of them the real effect of very early stage cracking is analyzed. Rossi *et al.* (2013) has underlined that in none of the existing theories, including micro-prestress one, but also in the concept of viscoplastic behavior of cement hydrates by Acker (2004) and in concept of rearrangement of nanoscale particles around limit packing densities by Vandamme *et al.* (2009) evolution of microcracking is not considered as the physical origin of concrete creep.

In our work we focus our attention on phenomenological description of concrete behavior strained during its maturing and conclusions drawn based on our research will be verified in laboratory tests. If our hypotheses are confirmed the next step will lead to more detailed, microstructural description. The paper is organized as follows. In Section 2 a detailed description of the model, including thermal, creep, irreversible straining effects and evolution of layers is

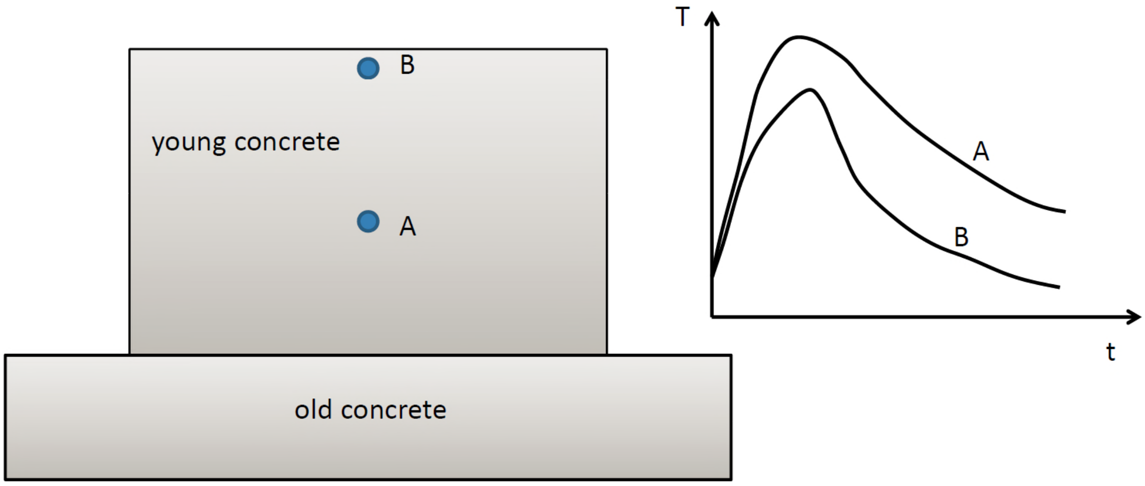

Fig. 1 Practical problem of block of young concrete resting on old concrete

given. In Section 3 results of two tests are presented, i.e. the 1D basic creep test for maturing concrete and then the 1D tensile tests conducted on concrete samples preloaded by compressive loading applied at stage of their maturing. Section 4 summarizes the paper.

2. Multi-layered model of aging concrete arbitrarily strained during its maturing

The analysis of stress/strain state in a system composed of a block of young concrete resting on a block of old concrete is one of the problems frequently met in the engineering practice. If the structure block is relatively massive then we may notice that the evolution of the thermal ($T(x,t)$) and shrinkage fields ($W(x,t)$) is different in certain zones of the structure. This effect is shown in Fig. 1.

If we took a look at the microstructure of concrete at early stage of its maturing, at the level of meso-scale we could observe that the effect of solidification takes place in cement paste but also at the skeleton-paste interfaces. This process is governed by the kinetics of chemical reactions. These reactions are highly exothermic causing strong increase of temperature in different parts of the structure. The current released heat H, described by the formula given below, is one of the measures used to control the level of solidification process

$$H(M) = H_\infty \frac{a\,M}{1 + a\,M} \tag{1}$$

$$M(t) = \int_{t_d}^{t} \exp\left(\frac{Q}{R}\left[\frac{1}{T_{ref}} - \frac{1}{T(\tau)}\right]\right) d\tau \tag{2}$$

In the above expressions the measure of current equivalent time is denoted by M (unit [days]), current value of released heat from unit volume by H (unit [J/m^3]), maximum released heat from unit volume by H_∞ (unit [J/m^3]), current absolute temperature by T (unit [K]), reference temperature by T_{ref}, activation energy by Q (unit [J/mol]), universal gas constant by R (unit [J/mol

K]), dormant time by t_d (unit [days]) and material property that parameterizes hyperbolic relation for $H(M)$ by a (unit [1/day]). The kinetics of chemical reactions is represented here by Eq. (2).

2.1 General concept of the model

The basic concept of the layered model (initially proposed by Szarliński and Truty (1994)) is such that any amount of heat released/discharged from a unit volume of concrete, in the course of hydration process of cement, is accompanied by the creation of new bonds between its particles. These bonds can be thought as fibers or chains, and those which are created at the same time instance form a layer which begins its own life as a solid concrete (this layer does not undergo any further growing in the future). In other words, each layer has got its own history of straining and possible damage and it contributes - together with other layers created earlier - to carrying overall stresses existing in the concrete at any time of maturing. At every time instance stresses arisen in each layer result from phenomenological properties of this layer, current total strain increment, identical for all the existing layers, and straining history of this layer. The main goal of our approach is to reuse any existing constitutive model formulated for the old concrete in our layered formulation and therefore a notion of effective stress in each layer has to be introduced. The i−th component of the stress vector $\vec{\mathbf{p}}$, corresponding to the intersection of the concrete body at a given point, by a plane defined through the external normal $\vec{\mathbf{n}}$, and carried out by all activated layers K=0..N_{act}−1, can be defined as follows (here we use tensorial notation)

$$p_i = \frac{\Delta F_i}{\Delta A} = \frac{\sum_{K=0}^{N_{act}-1} \Delta F_{K,i}}{\Delta A} = \frac{\sum_{K=0}^{N_{act}-1} \sigma_{K,ij}\, n_j\, w_K\, \Delta A}{\Delta A} = \sum_{K=0}^{N_{act}-1} \sigma_{K,ij}\, w_K\, n_j \tag{3}$$

In the above definition components of the global internal force vector and the one carried out by K-th layer are denoted by ΔF_i and $\Delta F_{K,i}$ respectively, the elementary global surface area is denoted by ΔA while term ($w_K \Delta A$) represents part of ΔA that is carrying out effective stresses of K-th layer. At this stage of our research we assume that at the end of the maturing process sum of weighting factors w_K (layer bond fractions) satisfies the following condition (N is the total number of layers that can be activated, arbitrarily assumed by the analyst)

$$\sum_{K=0}^{N-1} w_K = 1 \tag{4}$$

This condition does not need to be necessarily satisfied if we accept that in the case of macro-cracks appearing at the early stage of maturing new bonds may not be created due to excessive crack opening. This problem is already considered by the authors, but certain experiments must be carried out first to confirm our hypotheses. The most important consequence of Eq. (3) is that any implemented constitutive model can be used for the description of a given layer and therefore incremental constitutive law for maturing concrete can be defined as follows (here we use matrix notation)

$$\Delta\boldsymbol{\sigma} = \sum_{K=0}^{N_{act}-1} \Delta\boldsymbol{\sigma}_K\, w_K \tag{5}$$

$$\Delta\boldsymbol{\sigma}_K = \mathbf{D}^e\left(\Delta\boldsymbol{\varepsilon} - \Delta\boldsymbol{\varepsilon}_K^p - \Delta\boldsymbol{\varepsilon}_K^c - \Delta\boldsymbol{\varepsilon}^o\right) \tag{6}$$

In the above equations the effective stress increment in K−th layer is denoted by $\Delta\sigma_K$ and it is weighted by a corresponding weighting factor (layer bond fraction) w_K. As we can see total strain increment $\Delta\boldsymbol{\varepsilon}$ and increment of imposed strains $\Delta\boldsymbol{\varepsilon}^{\mathbf{o}}$ (due to thermal changes and shrinkage) are common for all existing layers while irreversible ($\Delta\boldsymbol{\varepsilon}_K^p$) and creep ($\Delta\boldsymbol{\varepsilon}_K^c$) strain increments are inherently connected to a given layer.

2.2 Procedure for layers activation

The most important aspect in the proposed layered model for concrete is related to the activation of layers in time. Before we start describing this crucial procedure we have to mention that each new layer is created in virgin state that is stress free. It results from 2-nd law of thermodynamics. In our approach at any point in the structure layers may be created with different rate. We assume that activation procedure is driven by current fraction of total released heat $\Delta H/H_\infty$. In order to avoid singularities due to zero stiffness, but also to reduce the error caused by step-wise activation of layers, we assume that the first layer is always active starting from the first time step after dormant time period t_d (time at which transition from liquid to solid state takes place). Well-designed procedure for layers activation, with their associated weights, is crucial, if smooth stress-strain characteristics are to be obtained. Therefore, we propose the following recurrent scheme for setting layer weights (index K starts from zero)

$$w_K = \min\left\{\left(\sum_{i=0}^{K-1} w_i\right), w_{\max}\right\}\cdot \varepsilon_{\mathrm{TOL}} \qquad \text{for} \quad K = 1..N-1 \tag{7}$$

The last weight is corrected to fulfill the condition that the sum of all weights is equal to one. This is achieved by using the correction formula

$$w_{N-1} = 1 - w_{N-2} \tag{8}$$

In this procedure we have to define the values of three parameters w_0, $\varepsilon_{\mathrm{TOL}}$ and $w_{\max}$. The weight of the first layer (that exists from the very beginning (K=0)) can be set as w_0=0.1 or w_0=0.2 for instance. Parameter $\varepsilon_{\mathrm{TOL}}$ is responsible for the reduction of the error caused by stepwise activation of layers in time. Therefore, the fraction of weight of each newly created layer and sum of weights of all already existing layers should be smaller than $\varepsilon_{\mathrm{TOL}}$. In addition, the maximum value of layer weight is bounded by $w_{\max}$ parameter. To put reasonable limit on the total number of layers to be activated, values of w_0, $\varepsilon_{\mathrm{TOL}}$ and $w_{\max}$ cannot be too small. One may assume $\varepsilon_{\mathrm{TOL}}$=0.1..0.2 and $w_{\max}$=w_0 for instance. Assuming w_0=0.2, $\varepsilon_{\mathrm{TOL}}$=0.2 and $w_{\max}$=0.2 we will get 10 layers with the following weights w_K ={0.200, 0.040, 0.048, 0.058, 0.069, 0.083, 0.100, 0.119, 0.143, 0.140}. In the next step activation maturities M_K must be set for each layer. The first one is activated at M_0 = 0 (by definition), while all the remaining ones are activated based on normalized relation $H(M)/H_{\mathrm{e}}(M)$, in which $H_{\mathrm{e}} = H(M(t_{\mathrm{end}}))$ is usually slightly smaller than H_∞ due to truncation of time axis of $H(M(t))$ curve. We assume that there exists strict correspondence between layers generation rate and the total amount of released heat due to hydration. This assumption leads to the following relation

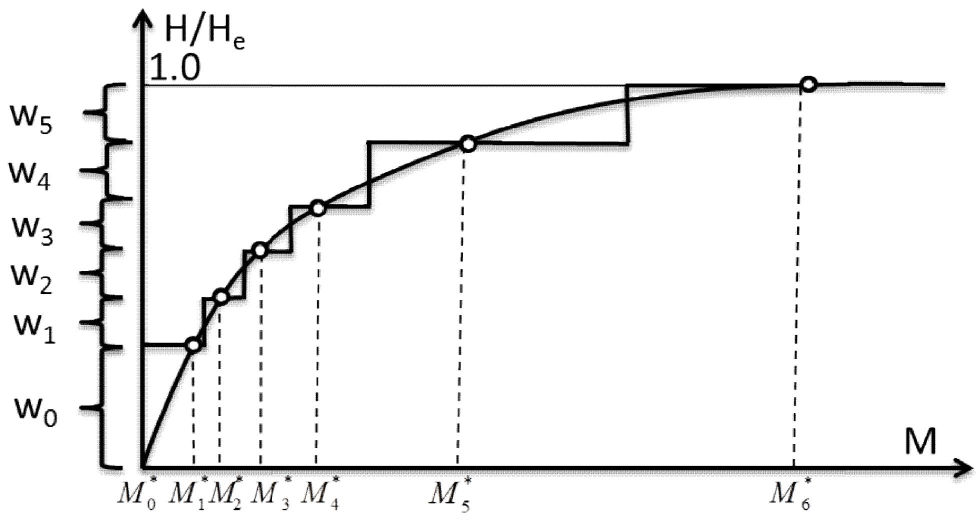

Fig. 2 Procedure for setting layer activation time/equivalent time

$$\sum_{K=0}^{N_{\text{act}}(M)-1} w_K = \frac{H(M)}{H_e} \tag{9}$$

where $N_{\text{act}}(M)$ is the current number of activated layers at current equivalent time value M. With this assumption we can identify characteristic equivalent time instances M_i^* (see Fig. 2) by interpolating $\frac{H}{H_e}(M)$ curve at each characteristic value of released heat due to hydration $\frac{H(M_i)}{H_e} = \sum_{K=0}^{i-1} w_K$ for each $i = 1..N - 1$. Later on activation equivalent time instances M_K are computed using midpoint rule as follows (N.B. $M_0^* = 0$)

$$M_K = \frac{1}{2}\left(M_K^* + M_{K+1}^*\right) \quad K = 1..N-1 \tag{10}$$

2.3 Inelastic behavior of nonaging concrete

At the current stage of our research we assume that instantaneous deformation of each layer is described by a simple elasto-plastic model with linear softening. Plasticity condition (Rankine law), flow rule and softening law are described by the following expressions

$$F(\boldsymbol{\sigma}_K) = \sigma_{1,K} - f_{ct} \le 0 \tag{11}$$

$$\Delta\boldsymbol{\varepsilon}_K^p = \Delta\lambda \frac{\partial F}{\partial \boldsymbol{\sigma}_K} \tag{12}$$

$$\Delta f_{ct} = H^{p}\ \Delta\boldsymbol{\varepsilon}^{p}_{1,K} \tag{13}$$

The expected tensile strength of concrete if it had not been damaged at stage of maturing is denoted here as f_{ct} and softening modulus as H^p. The value of softening modulus H^p can be related to the value of Young modulus E via coefficient α_{sf} as follows

$$H^{p} = -\alpha_{sf}\ E \tag{14}$$

2.3 Basic creep

The basic creep compliance function $J(t,t')$ proposed by Bažant and Kim (1991) seems to be sufficiently accurate to describe concrete behavior at each early age. It takes the following general form

$$J(t,t') = q_1 + F(\boldsymbol{\sigma})\left(q_2\ Q(t,t') + q_3\ \ln(1+\left(\frac{t-t'}{\lambda_o}\right)^{n}) + q_4\ ln\frac{t}{t'}\right) \tag{15}$$

In the Eq. (15) function $F(\boldsymbol{\sigma})$ is equal to unity for linear creep, the instantaneous compliance is represented by q_1 , aging viscoelastic one by q_2, nonaging viscoelastic by q_3 and viscous one by q_4 . Parameters λ_o and n are fixed to λ_o = 1 [days] and n = 0.1. Østegard *et al.* (2001) observed that Eq. (15) significantly undershoots basic creep for concrete loaded at very early stage (below 1 day). They proposed to replace q_2 parameter by the following function $\tilde{q}_2$

$$\tilde{q}_2 = q_2\,\frac{t'}{t' - q_5} \tag{16}$$

in which q_5 is interpreted as the transition time from viscoelastic fluid to viscoelastic solid behavior. Wei and Hansen (2013) amplified the q_4 parameter ($q_4 \approx 20.3(a/c)^{-0.7}$, where a/c is the aggregate-to-cement ratio) by an additional factor q_7 to obtain a good fit between theoretical compliance function and the empirical one indirectly derived from restrained strain-stress measurements.

Assuming that all material parameters appearing in $J(t,t')$ are known one may derive the expression for evolution of current stiffness modulus $E(t')$ at loading time t'

$$E(t') = J^{-1}(t' + \Delta t_o, t') \tag{17}$$

where Δt_o is usually assumed as 0.001 [days].

This function is not explicitly needed in our model, but we postulate that $E(t')/E_\infty \approx H(M(t'))/H_\infty$ (see Eq. (1) and (2)). In case when $T(t) = T_{ref}$ the equivalent time $M(t)$ becomes identical with time and one may easily optimize parameter a in Eq. (2). This expression can also be used to derive specific creep function $C(t,t')$ defined as follows

$$C(t,t') = J(t,t') - J(t' + \Delta t_o, t') \tag{18}$$

Taking into account the fact that each newly created layer is a non-aging one the $C(t,t')$ function can be expressed as follows

$$C(t,t^{'}) \approx \underbrace{q_3 \ln \frac{1+(t-t^{'})^n}{1+(\Delta t_o)^n}}_{C_{ve}(t,t^{'})} + \underbrace{q_4 \ln \frac{t}{t^{'}}}_{C_{vf}(t,t^{'})} \tag{19}$$

The first term C_{ve} (t,t') corresponds to the non-aging visco-elastic creep while the second one C_{vf} (t,t') to the viscous flow. These two terms require two different numerical algorithms to set the increment of creep strains. The visco-elastic term can be expressed by the following integral equation

$$\boldsymbol{\varepsilon}_K^{c,ve}(t) = \mathbf{D}_o^{-1} \int_{t_{o,K}}^{t} -\boldsymbol{\sigma}_K(t^{'}) \frac{\partial C_{ve}(t,t^{'})}{\partial t^{'}} \mathrm{d}t^{'} \tag{20}$$

$$\mathbf{D}_o = \frac{1}{E}\mathbf{D}^e \tag{21}$$

where effective stress in K–th layer is denoted by $\boldsymbol{\sigma}_K$ while Young modulus for old concrete by E (one may assume $E = E(28[\text{days}])$. In order to obtain an efficient recurrent formula for the increment of visco-elastic creep strains the specific creep function C_{ve} (t,t') is approximated by a series of Kelvin units which yields

$$C_{ve}(t,t^{'}) = \sum_{i=1}^{N_K} A_i \left(1 - e^{-(t-t^{'})/\tau_i}\right) \tag{22}$$

In the above expression N_K is the number of Kelvin units and τ_i are retardation times. In order to obtain good matching between $C_{ve}(t,t')$ (Eq. (22)) and $C_{ve}(t,t')$ (Eq. (19)) we must set proper number of Kelvin units N_K, retardation times τ_i and coefficients A_i . The typical approach is such that we assume retardation times τ_i first, using the rule $\tau_{i+1} = 10\,\tau_i$ with $\tau_1 = 0.005$ [days] and $\tau_{NK} > 2t_{\max}$ ($t_{\max}$ is the maximum prediction time period), and then we can minimize the following error functional E_R (A_i) (note that all A_i must be positive)

$$E_R(A_i) = \sum_{k=1}^{N_{t_k}} \left(\sum_{i=1}^{N_K} A_i \left(1 - e^{-(t_k-t^{'})/\tau_i}\right) - q_3 \ln \frac{1+(t_k-t^{'})^n}{1+(\Delta t_o)^n} \right)^2 \tag{23}$$

in which k is the index of time instance on digitized curve C_{ve} (t,t') and N_{t_k} is the number of digitized time instances. More elegant approach based on continuous retardation spectra was recently published by Jirásek and Havlásek (2014).

The recurrent formula for the increment of creep visco-elastic strains can be derived from the integral Eq. (20) by subtracting total visco-elastic creep strains at the two consecutive time instances n and $n-1$ as shown in Eq. (25)

$$\Delta\boldsymbol{\varepsilon}_{K,n}^{c,ve} = \mathbf{D}_o^{-1} \Delta\tilde{\boldsymbol{\varepsilon}}_{K,n}^{c,ve} \tag{24}$$

$$\Delta\tilde{\boldsymbol{\varepsilon}}^{c,ve}_{K,n} = \int_{t_{o,K}}^{t_n} -\boldsymbol{\sigma}_K(t')\frac{\partial C_{ve}(t_n,t')}{\partial t'}\mathrm{d}t' - \int_{t_{o,K}}^{t_{n-1}} -\boldsymbol{\sigma}_K(t')\frac{\partial C_{ve}(t_{n-1},t')}{\partial t'}\mathrm{d}t'$$

$$= \int_{t_{n-1}}^{t_n} -\boldsymbol{\sigma}_K(t')\frac{\partial C_{ve}(t_n,t')}{\partial t'}\mathrm{d}t' + \int_{t_{o,K}}^{t_{n-1}} -\boldsymbol{\sigma}_K(t')\frac{\partial C_{ve}(t_n,t')}{\partial t'}\mathrm{d}t' \tag{25}$$

$$-\int_{t_{o,K}}^{t_{n-1}} -\boldsymbol{\sigma}_K(t')\frac{\partial C_{ve}(t_{n-1},t')}{\partial t'}\mathrm{d}t'$$

The final form of this recurrent formula can be expressed as follows

$$\Delta\tilde{\boldsymbol{\varepsilon}}^{c,ve}_{K,n} = \sum_{i=1}^{N_K}\Delta^i\tilde{\boldsymbol{\varepsilon}}^{c,ve}_{K,n} \tag{26}$$

$$\Delta^i\tilde{\boldsymbol{\varepsilon}}^{c,ve}_{K,n} = \left(e^{-\Delta t_n/\tau_i}-1\right){}^i\tilde{\boldsymbol{\varepsilon}}^{c,ve}_{K,n-1} + \left(\boldsymbol{\sigma}_{n-1}+\theta\Delta\boldsymbol{\sigma}_n\right)A_i\left(1-e^{-\Delta t_n/\tau_i}\right) \tag{27}$$

In order to derive the increment of viscous creep strains we have to assume a certain formula for the viscosity coefficient $\eta_{f,K}$ in each active layer. To preserve the qualitative similarity of viscous creep term in the solidification model and the presented one we propose the following formula for $\eta_{f,K}$

$$\eta_{f,K} = \frac{t-t_{o,K}+\xi}{q_4} \tag{28}$$

in which ξ is a parameter (unit [days]) that has to be optimized. Its value can approximately be set to $\xi \approx 2\, q_5$.

Based on the above definition the increment of viscous creep strains can be expressed as follows

$$\Delta\tilde{\boldsymbol{\varepsilon}}^{c,vf}_{K,n} = q_4\left(\boldsymbol{\sigma}_{n-1}+\theta\Delta\boldsymbol{\sigma}_n\right)\ln\frac{t_n-t_{o,K}+\xi}{t_{n-1}-t_{o,K}+\xi} \tag{29}$$

$$\Delta\boldsymbol{\varepsilon}^{c,vf}_{K,n} = \mathbf{D}_o^{-1}\Delta\tilde{\boldsymbol{\varepsilon}}^{c,vf}_{K,n} \tag{30}$$

By comparing solidification model and the presented one a slightly different viscous creep strain state is expected for concrete loaded at the early age. For larger time values a relatively good match will be observed (if no early age cracking is observed).

By taking into account both derived expressions for visco-elastic and viscous creep strain increments the incremental constitutive equation (see Eq. (6)) can be rewritten in the following form

$$\Delta\boldsymbol{\sigma}_{K,n} = \tilde{\mathbf{D}}^{\mathrm{e}}\left(\Delta\boldsymbol{\varepsilon}_n - \Delta\boldsymbol{\varepsilon}^{p}_{K,n} - \Delta\boldsymbol{\varepsilon}^{c}_{K,n} - \Delta\boldsymbol{\varepsilon}^{o}_{n}\right) \tag{31}$$

where

$$\Delta\boldsymbol{\varepsilon}^{c}_{K,n} = \Delta\boldsymbol{\varepsilon}^{c,ve}_{K,n} + \Delta\boldsymbol{\varepsilon}^{c,vf}_{K,n} \tag{32}$$

and

$$\tilde{\mathbf{D}}^{\mathrm{e}} = \frac{\mathbf{D}^{\mathrm{e}}}{1+\theta\, E\left(\sum_{i=1}^{N_K} A_i\left(1-e^{-\Delta t_n/\tau_i}\right) + q_4\, \ln\dfrac{t_n - t_{o,K} + \xi}{t_{n-1} - t_{o,K} + \xi}\right)} \tag{33}$$

3. Numerical examples

The two test cases are analyzed in this section. In the first one the basic tensile creep test for an aging concrete is reproduced based on the experimental data published by Østegard *et al.* (2001). In the second one an effect of initial compressive preloading in maturing period on final tensile strength of fully matured concrete is analyzed.

3.1 Basic creep test by Østegard et al. (2001)

The cited tensile creep tests were carried out in the experimental setup developed by Østegard *et al.* (2001) on dog bone-shaped concrete specimens. During experimental work all specimens were cured and tested at a constant temperature 23°C and relative humidity 50% RH. In the worked out procedure the effect of drying shrinkage was negligible while equivalent time *M*, because of constant temperature, was strictly proportional to the age. Results and data for Østegard's creep tests 1..4 carried out for composition of concrete mix A were used to verify capabilities of our model. Østegard at al. have shown that the standard solidification theory by Bažant is unable to reproduce basic creep once the loading is applied at *t'* below 1 day. Therefore they introduced the correction to q_2 term (see Eq. (16)) in the compliance function expressed by Eq. (15). For sake of clarity we will recall the complete set of expressions describing basic creep compliance function *J*(*t,t'*) used by Østegard *et al*.

$$J(t,t') = q_1 + \tilde{q}_2\, Q(t,t') + q_3\, \ln(1+\left(t-t'\right)^{0.1}) + q_4\, ln\frac{t}{t'} \tag{34}$$

$$Q(t,t') = Q_f(t')\left[1+\left(\frac{Q_f(t')}{Z(t,t')}\right)^{r}\right]^{-1/r} \tag{35}$$

$$Q_f(t') = \left[0.086(t')^{2/9} + 1.21(t')^{4/9}\right]^{-1} \tag{36}$$

$$Z(t,t') = (t')^{-1/2} \ln\left[1 + (t - t')^{0}.1\right] \tag{37}$$

$$r = 1.7\,(t')^{0.12} + 8 \tag{38}$$

$$\tilde{q}_2 = q_2 \frac{t'}{t' - q_5} \tag{39}$$

The best fit between the theory and experimental results was obtained by Østegard *et al*. for $q_1 = 6.7\cdot10^{-6}$ MPa^{-1}, $q_2 = 16.6\cdot10^{-6}$ MPa^{-1}, $q_3 = 47.1\cdot10^{-6}$ MPa^{-1}, $q_4 = 28.3 \cdot 10^{-6}$ MPa^{-1} and $q_5 = 0.59$ [days]. Basing on the optimized set of parameters $q_1..q_5$ one may derive the formula for current standard Young modulus at a given loading time instance t' using the definition expressed by Eq. (17). If we assume $t_d = q_5$ and T_{ref} = 23°C then the current equivalent time (see Eq. (2)) will be equal to $M(t) = t - q_5$. Therefore the resulting (from our model) current equivalent stiffness modulus can be expressed as follows (see Eq. (1))

$$E(t') = E(28)\frac{a\,(t' - q_5)}{1 + a\,(t' - q_5)} \tag{40}$$

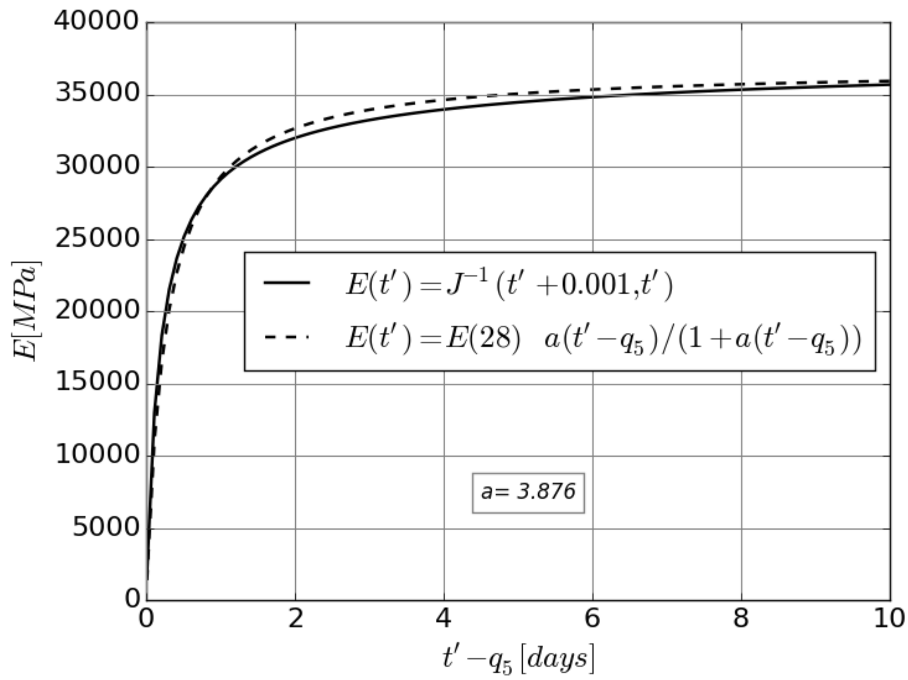

Fig. 3 Evolution of standard Young moduli in time according to experimental data by Østegard *et al.* (2001)

Table 1 Optimized set of parameters of 6 Kelvin units

Kelvin unit	1	2	3	4	5	6
τ_i [days]	0.005	0.05	0.5	5.0	50.0	500.0
$A_i \times 10^6$ [MPa]$^{-1}$	3.433	4.647	5.030	5.637	6.791	5.767

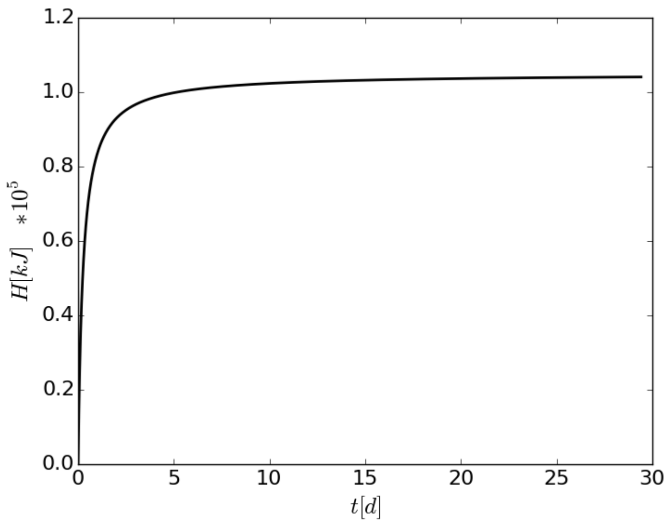

Fig. 4 Released heat *H(t)* time history at constant temperature T=23^o

The best fit between predicted $E(t')$ moduli from Østegard's and our model is obtained for a = 3.876 [days]$^{-1}$ (see Fig. 3). It is worth to mention that the optimal a value was obtained by minimizing the error functional in time range t' =q_5..q_5+2 [days].

As the aging effect in our model is included by means of activation of layers in time then the term q_2 $Q(t,t')$ is neglected by definition. Term related to q_3 parameter in the compliance function $J(t,t')$ is partly embedded in the visco-elastic creep measure and partly in the standard Young modulus. On the other hand q_1 is fully embedded in the current standard Young modulus value. The visco-elastic creep measure in our model is approximated by series of 6 Kelvin units with the optimized set of parameters (see Eq. (23)) given in Table 1.

The data set of material parameters used to calibrate our model is as follows E = 36850 MPa, ν = 0.2, visco-elastic creep parameters are given in Table1, t_d = 0.59 [days] (same as q_5), a = 3.876 [days], T_{ref} = 23°C, f_{ct} = 2.8 MPa, $\alpha = 10^{-5}$ °C^{-1}, H_∞ =105000 kJ/m^3, Q/R = 4000 K at every time instance. As it was already mentioned this tensile creep test is conducted under constant temperature and humidity and therefore thermal properties are not meaningful. The ratio between applied tensile stress and current tensile strength is kept constant and equal to 0.45. Hence strength parameters are not meaningful either. The released heat time history is shown in Fig. 4, respectively. In the experiments the tensile traction was applied to the samples at time instances t' = {0.67, 1.0, 3.0, 5.0} [days]. As the setting time was approximately equal to q_5 = 0.59 [days] therefore real loading time instances in our model are t' = {0.08, 0.41, 2.41, 4.41} [days]. In order to show the role of the initial weight w_0 our predictions were made for three pairs of (w_0,ε_{TOL}) parameters: (w_0 = 0.2, ε_{TOL} = 0.2), (w_0 = 0.25, ε_{TOL} = 0.2), (w_0 = 0.15, ε_{TOL} = 0.15).

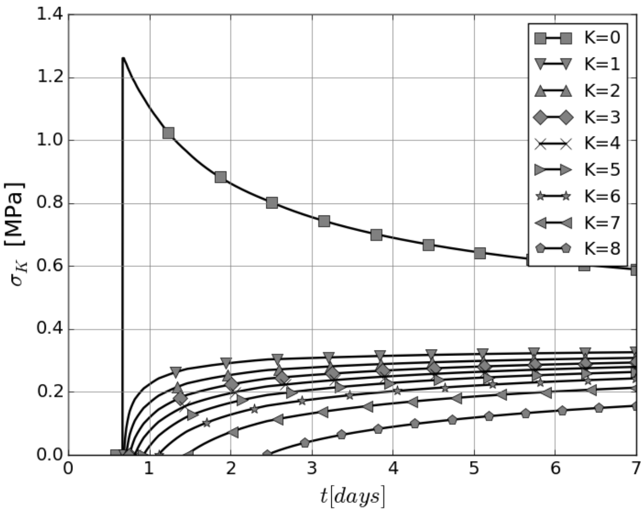

Fig. 5 Effective stress time histories for loading time instance *t'* = 0.67 [days] and w_0 = 0.25, ε_{TOL} = 0.2

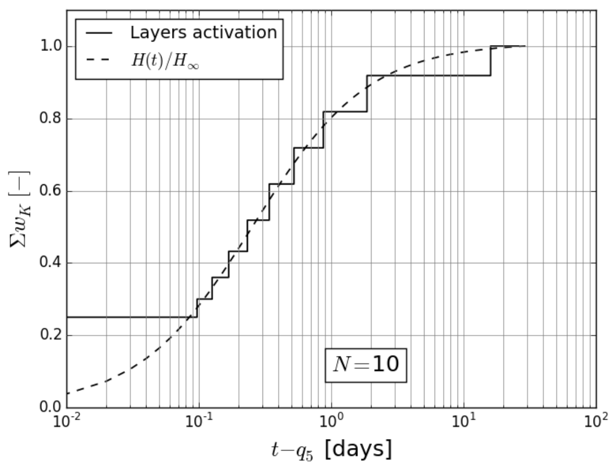

Fig. 6 Time history of layers activation w_0 = 0.25 and ε_{TOL} = 0.2

For better understanding how the proposed model reproduces the basic creep at the early stage let us analyze first the effective stress time histories in all layers for case when load is applied at *t* = 0.67 [days], while w_0 = 0.25 and ε_{TOL} = 0.2 (see Fig. 5). As we can see in layer "0" stress is constant but then right after appearance of the second layer it starts to relax. Because of the continuous creep of the existing layers the newly created ones become stressed.

The resulting time history of layers activation (10 layers) for w_0=0.25 and ε_{TOL}=0.2 is shown in Fig. 6. The resulting compliance functions *J*(*t*,*t'*) for all three analysed cases are shown in Figs 7, 8 and 9 respectively. We can notice that for loading time instances starting from 1 [day] the initial weight w_0 does not play any important role and results from our model and from the modified (by

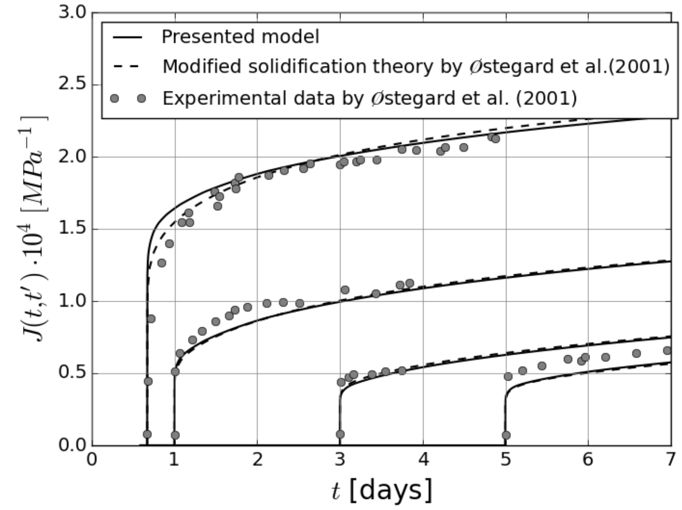

Fig. 7 Compliance functions $J(t,t')$ for w_0 = 0.2 and ε_{TOL} = 0.2

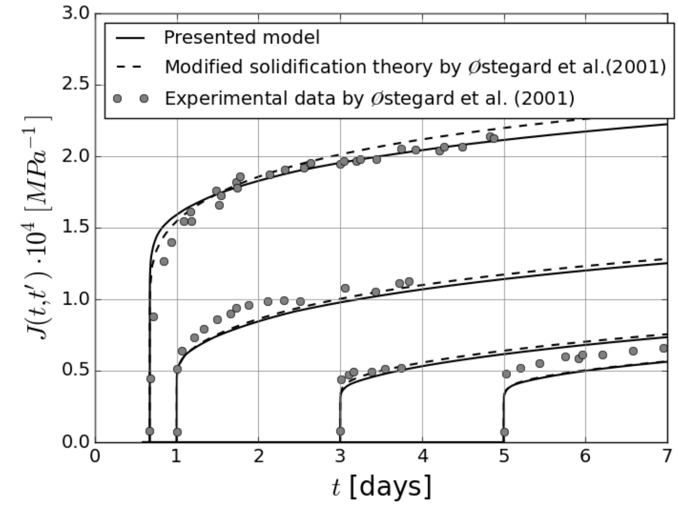

Fig. 8 Compliance functions $J(t,t')$ for w_0 = 0.25 and ε_{TOL} = 0.2

term q_5) solidification one are almost the same. On the other hand very good agreement between the experiment and the model for loading time instance t' = 0.67 [days] (t' = 0.08 [days] in our model) is achieved for w_0 = 0.25. We should mention here that in the experiment by Østegard *et al.* (2001) an important influence of the stress to current strength ratio was observed. The general trend was such that for higher stress to strength ratio higher creep strains were measured. This phenomenon can be reproduced by modifying the viscous creep term in which current viscosity should not only be time but also stress dependent.

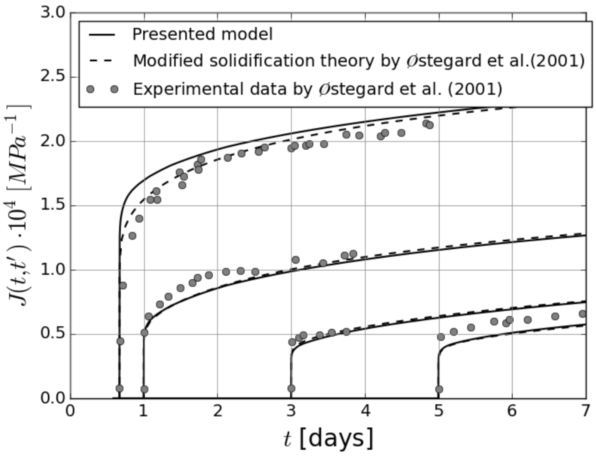

Fig. 9 Compliance functions $J(t,t')$ for $w_0 = 0.15$ and $\varepsilon_{\mathrm{TOL}} = 0.15$

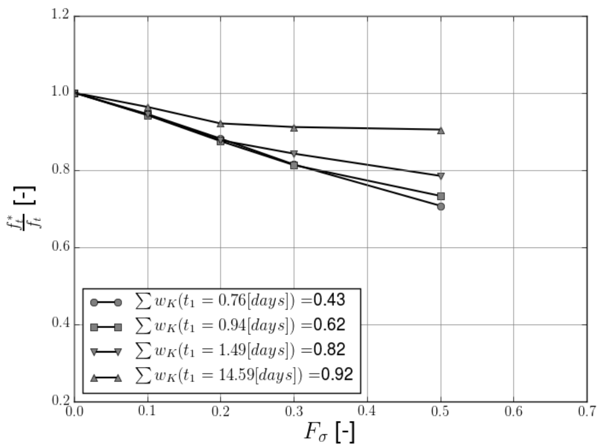

Fig. 10 Reduction of peak tensile strength due to initial compressive preloading (creep active)

3.2 Tensile strength of a concrete sample preloaded at stage of its maturing

In this example we analyze a concrete sample, made of fresh concrete, subjected first to the constant compression loading program, carried out in the time period $t_1..t_2$, then switched to the displacement control one, in which the sample is elongated until complete loss of tensile bearing capacity. The compression loading history is described by the following formula

$$\sigma(t) = 0 \quad \text{for} \quad t \le t_1 \tag{41}$$

$$\sigma(t) = F_\sigma \ f_c(t_1) \quad \text{for} \quad t = t_1..t_2 \tag{42}$$

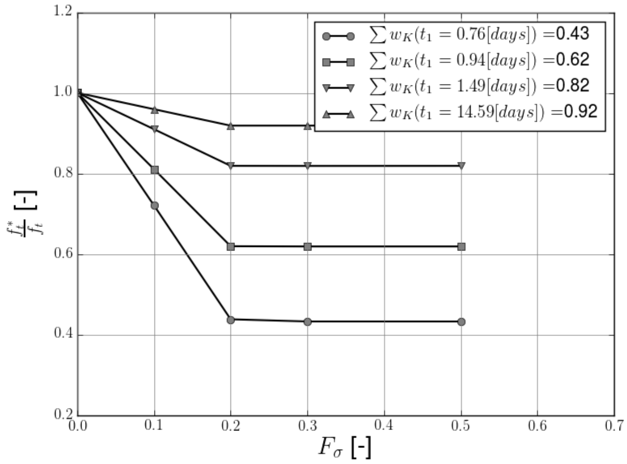

Fig. 11 Reduction of peak tensile strength due to initial compressive preloading (creep inactive)

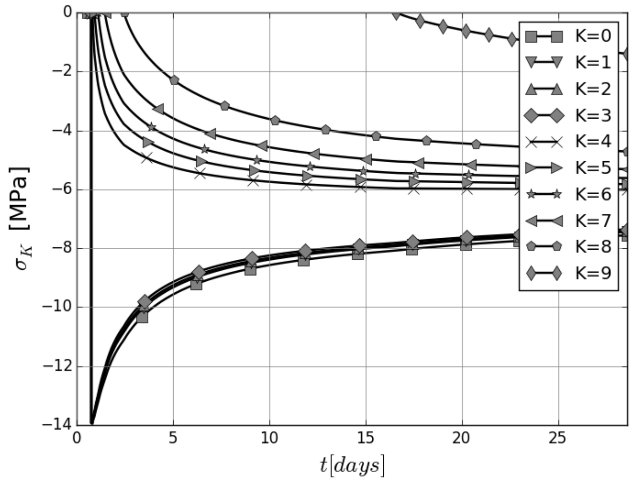

Fig. 12 Effective stress time histories during compressive preloading applied at t_1 = 0.76 [days] at loading level F_σ = 0.5 (creep active)

where F_σ is an assumed applied stress to current strength (at time t_1) ratio.

In this example we consider four values of loading time instances t_1 = 0.76, 0.94, 1.49, 14.59 [days] (the real loading time in the model is reduced by q_5=0.59 [day]) and five levels of compressive preloading F_σ = 0.0, 0.1, 0.2, 0.3, 0.5. The aforementioned loading time instances t_1 (measured starting from the setting time) correspond to the following levels of solidification $\Sigma w_K(t_1)$ = 0.43, 0.62, 0.82, 0.92. All material properties are taken from the previous example (basic creep test) while w_0 = 0.25, ε_{TOL} = 0.2 and w_{max}=0.1. No distinction between tensile and compression creep is made here. For sake of the quantitative comparison inviscid case is also

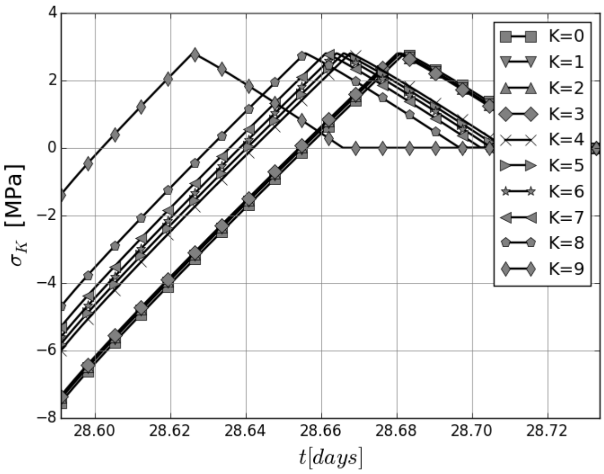

Fig. 13 Effective stress time histories during tensile kinematic loading preceded by the compressive preloading applied at t_1 = 0.76 [days] at loading level F_σ = 0.5 (creep active)

considered (viscoelastic and viscous creep are neglected). As it is shown in Figs. 10 and 11 we observe a significant reduction of the resulting peak tensile strength f_t^* that is influenced by the value of compressive preloading and its application time (*t'*). Restricting our attention to the case with visco-elastic and viscous creep active we may observe that the loss of the tensile bearing capacity may reach 30% of its nominal value. By analyzing this plot we can conclude that earlier compressive preloading and larger magnitude of that preloading, both lead to larger reduction of tensile bearing capacity. Similar effect is observed in the fully inviscid case where reduction of tensile bearing capacity is definitely higher and tending faster to the asymptotic value with the magnitude of applied compressive preloading. The maximum deduced reduction in the inviscid case is about twice higher than in the case when creep is considered.

In order to understand why this reduction is induced by the model let us analyze the time history of effective stresses in all layers, first in the period of compressive preloading and then during tensile test for the case with creep active. The corresponding time histories of effective stresses in the stage of compression is shown in the Fig. 12 while the tensile one is shown in the Fig. 13. As we can see those layers that were existing before compressive load application are creeping until new layers appear. Starting from that time they start relaxing. As the strain increments are the same for all existing layers therefore we observe a certain form of effective stress redistribution among the layers. Newly created layers, that are stress free at the beginning, become stressed, although largest effective stress are still observed in the oldest layers. By switching to the fast kinematic loading program in each layer we have a different initial effective stress $\boldsymbol{\sigma}_K$. Therefore, during kinematically induced tension the youngest layers will start to soften first. This effect is well visible in Fig. 13. Each layer reaches its maximum tensile bearing capacity at different time. Hence the resulting global peak tensile strength must be reduced. It is worth to mention that creep phenomenon in compression is usually stronger from the one in tension, therefore the resulting tensile strength loss can be smaller. However, it is absolutely obvious that this detected phenomenon requires a careful experimental testing for its confirmation and then model enhancements, if needed.

The minimal set of laboratory experiments carried out on ϕ16 cylinders should include three series of compressive preloading stress levels i.e. 0.0 f_c (t=1 day), 0.2 f_c (t=1 day) and 0.4 f_c (t=1 day), applied approximately 1 day after setting the samples. Constant ambient humidity and temperature should be preserved during the tests. Samples subject to the compressive load application should be notched first (about 10 mm) and then, after 28 days, should be elongated until the maximum tensile bearing capacity is reached.

4. Conclusions

A general framework for the description of stress-strain relations for concrete at the stage of its maturing is proposed in the paper. The multilayer approach in which the activation of layers is driven by the progress of cement hydration allows one to apply any suitable constitutive law for each distinct layer. Therefore, no explicit dependency of stiffness moduli or strength on time is needed. The aging effect is hidden in the discontinuous in time process of growth of solidified layers. The additional viscous creep present in the standard solidification theory was introduced at the layer level assuming that current viscosity parameter is time dependent and it takes into account layer activation time. The two analyzed numerical examples show that the model can properly describe the effect of the aging and creep. It is important that our model can give very good predictions for loading time instances just after the setting time. A relatively simple, yet good enough for the considered test cases, constitutive model was used for each layer although we want to underline once more that our framework accepts any currently available constitutive model developed for description of the old concrete behavior. The second analyzed numerical example shows that compressive preloading of concrete during the stage of its maturing may reduce the final tensile strength. This reduction is strongly dependent on the age at which compressive loading is applied, and its history. This theoretical hypothesis requires comprehensive laboratory tests to be carried out for its confirmation and we are in the stage of their design and preparation. The detected phenomenon, to our best knowledge, was not investigated yet. Therefore the intuitive judgment can be risky in the analyzed case. From the practical point of view the proposed model will always lead to safer predictions by taking into account certain level of tensile strength loss due to initial compressive preloading. This can be crucial in designing massive RC structures, in which shear reinforcement is not required by the standards (EC2 for instance). However, we do underline once more that experiment can be the only way to confirm or falsify this intuitively unexpected result.

We believe that the proposed model will help to explain certain phenomena observed in prestressed concrete structures, like water tanks, but also in massive concrete structures (like large foundation rafts), in which early stage cracking is frequently observed.

The multi-dimensional applications, including regularization of strain localization, will be published by the authors in the nearest future.

References

Acker, P. (2004), "Swelling, shrinkage and creep: a mechanical approach to cement hydration", *Mater. Struct.*, **37**(4), 237-243.

Bažant Z. and Kim J.K. (1991), "Improved prediction model for time-dependent deformations of concrete: Part 2 - basic creep", *Mater. Struct.*, **24**(144), 409-421.

Bažant Z. and Prasannan S. (1989), “Solidification theory for concrete Creep. I: Formulation”, *J. Eng. Mech.*, **115**(8), 1691-1703.

Bažant Z. and Prasannan S. (1989), “Solidification theory for concrete creep. II: Verification”, *J. Eng. Mech.*, **115**(8), 1704-1725.

Bažant, Z., Hauggard A.B., Baweja, S. and Ulm F.J. (1997), “Microprestress-solidification theory for concrete creep. I: Aging and drying effects”, *J. Eng. Mech.*, **123**(11), 1188-1194.

Bažant, Z., Hauggard A.B., Baweja, S. and Ulm F.J. (1997), “Microprestress-solidification theory for concrete creep. II: Algorithm and verification”, *J. Eng. Mech.*, **123**(11), 1195-1201.

Gawin, D., Pesavento, F. and Schrefler B.A. (2006), “Hygro-thermo-chemo-mechanical modeling of concrete at early ages and beyond. Hygro-thermo-chemo-mechanical modeling of concrete at early ages and beyond. Part II: Shrinkage and creep of concrete”, *Int. J. Numer. Meth. Eng.*, **67**(3), 332-363.

Gawin, D., Pesavento, F. and Schrefler, B.A. (2006), “Hygro-thermo-chemo-mechanical modeling of concrete at early ages and beyond. Part I: Hydration and hygro-thermal phenomena”, *Int. J. Numer. Meth. Eng.*, **67**(3), 299-331.

Hassanizadeh, M. and Gray, W.G. (1979), “General conservation equations for multiphase systems: 1 Averaging procedure”, *Adv. Water Resour.*, **2**, 131-144.

Havlásek, P. (2012), “Modeling of concrete creep based on microprestress-solidification theory”, *Proceedings of the 9th fib International PhD Symposium in Civil Engineering: Karlsruhe Institute of Technology (KIT)*, Karlsruhe, Germany, July (p. 453).

Havlásek, P. (2014), “Creep and shrinkage of concrete subjected to variable environmental conditions”, Ph.D. Dissertation, Czech Technical University in Prague, Prague.

Havlásek, P. and Jirásek, M. (2012), “Modeling of concrete creep based on microprestress-solidification theory”, Acta Politechnica, 52, 34-42.

Jirásek, M. and Havlásek, P. (2014), “Accurate approximations of concrete creep compliance functions based on continuous retardation spectra”, *Comput. Struct.*, **135**, 155-168.

Mabrouk, R., Ishida, T. and Maekawa, K. (2004), “A unified solidification model of hardening concrete composite for predicting the young age behavior of concrete”, *Cement Concrete Compos.*, **26**(5), 453-461.

Mihashi, H. and Nishiwaki, T. (2012), “Development of engineered self-healing and self-repairing concrete-state-of-the-art report”, *J. Adv. Concrete Tech.*, **10**(5), 170-184.

Østegard Z., Lange D.A., Altoubat S.A. and Stang H. (2001), “Tensile basic creep of early age concrete under constant load”, *Cement Concrete Res.*, **31**(12),1895-1899.

Rossi, P., Tailhan, J.L. and Le Maou, F. (2013), “Comparison of concrete creep in tension and in compression: Influence of concrete age at loading and drying conditions”, *Cement Concrete Res.*, **51**, 78-84.

Szarliński, J. and Truty, A. (1993), “Multilaminate non-linear model for cracked aging concrete”.

Vandamme, M. and Ulm, F.J. (2009), “Nanogranular origin of concrete creep”, *Proceedings of the National Academy of Sciences of the United States of America*, 106-26, 10552-10557.

Wei, Y. and Hansen, W. (2013), “Tensile creep behavior of concrete subject to constant restraint at very early ages”, *J. Mater. Civil Eng.*, **25**(9), 1277-1284.

Witakowski, P. (1998), “Thermodynamic theory of aging. Application to massive concrete structures” (in Polish), Zeszyty Naukowe Politechniki Krakowskiej, Nr 1.

AW